

Contents lists available at ScienceDirect

Physics Letters B

www.elsevier.com/locate/physletb

Revisiting electroweak phase transition in the standard model with a real singlet scalar

Cheng-Wei Chiang^{a,b,c}, Yen-Ting Li^a, Eibun Senaha^{d,*}^a Department of Physics, National Taiwan University, Taipei 10617, Taiwan^b Institute of Physics, Academia Sinica, Taipei 11529, Taiwan^c Kavli IPMU, University of Tokyo, Kashiwa, 277-8583, Japan^d Center for Theoretical Physics of the Universe, Institute for Basic Science (IBS), Daejeon 34126, Republic of Korea

ARTICLE INFO

Article history:

Received 11 August 2018

Received in revised form 10 December 2018

Accepted 10 December 2018

Available online 11 December 2018

Editor: M. Trodden

ABSTRACT

We revisit the electroweak phase transition in the standard model with a real scalar, utilizing several calculation methods to investigate scheme dependences. We quantify the numerical impacts of Nambu–Goldstone resummation, required in one of the schemes, on the strength of the first-order electroweak phase transition. We also employ a gauge-independent scheme to make a comparison with the standard gauge-dependent results. It is found that the effect of the Nambu–Goldstone resummation is typically $\sim 1\%$. Our analysis shows that both gauge-dependent and -independent methods give qualitatively the same result within theoretical uncertainties. In either methods, the scale uncertainties in the ratio of critical temperature and the corresponding Higgs vacuum expectation value are more than 10%, which signifies the importance of higher-order corrections.

© 2018 The Author(s). Published by Elsevier B.V. This is an open access article under the CC BY license (<http://creativecommons.org/licenses/by/4.0/>). Funded by SCOAP³.

1. Introduction

Cosmic baryon asymmetry [1] is one of the longstanding problems in particle physics and cosmology. Though the standard model (SM) can satisfy the so-called the Sakharov criteria [2] in principle, the discovered Higgs boson with a mass of 125 GeV [3] is incompatible with successful electroweak baryogenesis (EWBG) [4] since the electroweak phase transition (EWPT) is a smooth crossover [5] rather than first order with expanding bubbles. It is known that this drawback can be easily circumvented by augmenting the minimal Higgs sector. The simplest extension is to add an $SU(2)_L$ singlet scalar, which provides not only a strong first-order EWPT but also a dark matter candidate if a Z_2 symmetry is imposed [6,8–13].

A thorny problem in investigating EWPT using a perturbative effective potential is the dependence on a gauge fixing parameter ξ [14,15] (for recent studies, see, e.g., Refs. [16,17]). For instance, the Higgs vacuum expectation value (VEV) obtained by the effective potential can change with a varying ξ . Such an unwanted ξ dependence eventually contaminate a baryon-number preserving criterion: $v_C/T_C \gtrsim 1$, where T_C denotes the critical tempera-

ture associated with the phase transition and v_C is the doublet Higgs VEV at T_C . As a result, any phenomenological consequences derived from this criteria suffer from the ξ dependence and are therefore unreliable unless the dependence can be kept under control.

Common lore is that if the EWPT is driven by scalar thermal loops or a tree-potential barrier, the ξ dependence is expected to be small. As found in the Abelian–Higgs model with an additional scalar [18], however, such an expectation is not always correct. It is concluded that the ξ dependence can be pronounced even when the tree-potential barrier exists. Nevertheless, this point is often overlooked in previous studies on the EWPT in the SM with a real singlet scalar.

Another issue is the occurrence of IR divergences in the effective potential in the R_ξ gauge with $\xi = 0$. For example, if the Higgs boson mass is renormalized using the one-loop effective potential in such a way that the loop corrections do not modify the tree-level mass relations,¹ the second derivative of the one-loop effective potential is ill-defined due to the IR divergences coming from the Nambu–Goldstone (NG) boson loops. One of the prescriptions for the problem is to resum higher-order corrections to the

* Corresponding author.

E-mail addresses: chengwei@phys.ntu.edu.tw (C.-W. Chiang), R04222022@ntu.edu.tw (Y.-T. Li), senaha@ibs.re.kr (E. Senaha).<https://doi.org/10.1016/j.physletb.2018.12.017>0370-2693/© 2018 The Author(s). Published by Elsevier B.V. This is an open access article under the CC BY license (<http://creativecommons.org/licenses/by/4.0/>). Funded by SCOAP³.¹ This is called “on-shell” renormalization in Ref. [8]. Since it is not the genuine on-shell renormalization, we refer to it as “on-shell-like” renormalization in the current paper.

NG masses [19,20]. One can show that the NG contributions have little effect on the Higgs mass once they are resummed. Nonetheless, it would be desirable to quantify their numerical impact on v_C/T_C explicitly.

In this paper, we revisit EWPT in the SM with a singlet scalar, focusing on the aforementioned two issues as well as the scheme dependence. We first clarify the numerical importance of the thermal gauge boson loops on v_C/T_C by subtracting them off from the finite-temperature effective potential in the Landau gauge $\xi = 0$. Even though this simple method cannot precisely quantify the ξ dependence, it tells how important the thermal gauge loops can be in order to achieve a strong first-order EWPT, especially $v_C/T_C \simeq 1$. We regard this as a simple criterion whether a further investigation of the ξ dependence is needed or not.

In addition to the numerical studies of v_C/T_C in the on-shell (OS)-like scheme with the NG resummation, we also evaluate v_C/T_C utilizing the following three methods commonly adopted in the literature for comparison: (1) the $\overline{\text{MS}}$ scheme, (2) the high-temperature (HT) potential defined as the tree-level potential plus thermal masses and (3) the Patel–Ramsey–Musolf (PRM) scheme [16]. In the first method, the tree-level NG boson masses are not zero in the one-loop corrected vacuum so that the NG resummation mentioned above is not required. The second method is manifestly gauge invariant since the thermal masses do not have the ξ dependence. In the last one, the Nielsen–Fukuda–Kugo (NFK) identity [22,23] is used to obtain the gauge-invariant T_C , and v_C is determined by use of the HT potential. We confine ourselves to $\mathcal{O}(\hbar)$ calculations in which the thermal resummation is not performed. Going beyond this order requires two-loop contributions as well, which is out of the scope of current investigation. Application of the $\mathcal{O}(\hbar)$ PRM scheme to the SM with a complex scalar can be found in Ref. [24]. However, devoted numerical comparisons between this scheme and the standard gauge-dependent ones are not performed. One of the goals of this study is to complement this part.

The paper is organized as follows. In Sec. 2, we introduce the model and define our notation. Renormalization schemes are given to fix the input parameters. In Sec. 3, we outline the EWPT in the model. Sec. 4 shows the results of our numerical analyses. The conclusion and discussions are given in Sec. 5.

2. Model

We consider a model in which an $SU(2)_L$ singlet real scalar S is added to the SM. The S boson can be a dark matter candidate if a Z_2 symmetry is imposed [11]. The tree-level Higgs potential with the Z_2 symmetry is then cast into the form:

$$V_0(H, S) = -\mu_H^2 H^\dagger H + \lambda_H (H^\dagger H)^2 - \frac{\mu_S^2}{2} S^2 + \frac{\lambda_S}{4} S^4 + \frac{\lambda_{HS}}{2} H^\dagger H S^2. \quad (1)$$

The doublet Higgs field is parametrized as

$$H(x) = \begin{pmatrix} G^+(x) \\ \frac{1}{\sqrt{2}} [v + h(x) + iG^0(x)] \end{pmatrix}, \quad (2)$$

where $v \simeq 246$ GeV denotes the VEV, h the 125-GeV Higgs boson, and $G^{0,\pm}(x)$ the NG bosons.

The tadpole conditions at tree level are

$$\begin{aligned} T_h &\equiv \left\langle \frac{\partial V_0}{\partial h} \right\rangle = v \left[-\mu_H^2 + \lambda_H v^2 + \frac{\lambda_{HS}}{2} v_S^2 \right] = 0, \\ T_S &\equiv \left\langle \frac{\partial V_0}{\partial S} \right\rangle = v_S \left[-\mu_S^2 + \lambda_S v_S^2 + \frac{\lambda_{HS}}{2} v^2 \right] = 0, \end{aligned} \quad (3)$$

where the symbol $\langle \dots \rangle$ means that the quantity sandwiched by the angled brackets is evaluated in the vacuum, and $v_S = \langle S \rangle$. The Z_2 -invariant vacuum corresponds to the solution: $\mu_H^2 = \lambda_H v^2$ and $v_S = 0$, from which the scalar boson masses are given by

$$\begin{aligned} m_h^2 &= -\mu_H^2 + 3\lambda_H v^2 = 2\lambda_H v^2, \\ m_S^2 &= -\mu_S^2 + \frac{\lambda_{HS}}{2} v^2. \end{aligned} \quad (4)$$

Denoting the background fields of H and S as $\varphi/\sqrt{2}$ and φ_S , respectively, the tree-level effective potential takes the form

$$V_0(\varphi, \varphi_S) = -\frac{\mu_H^2}{2} \varphi^2 + \frac{\lambda_H}{4} \varphi^4 + \frac{\lambda_{HS}}{4} \varphi^2 \varphi_S^2 - \frac{\mu_S^2}{2} \varphi_S^2 + \frac{\lambda_S}{4} \varphi_S^4. \quad (5)$$

To avoid an unbounded-from-below potential, one has to have $\lambda_H > 0$ and $\lambda_S > 0$, and additionally $-2\sqrt{\lambda_H \lambda_S} < \lambda_{HS}$ if $\lambda_{HS} < 0$. As far as the strong first-order EWPT is concerned, $\lambda_{HS} > 0$ is necessary so that the last condition is irrelevant in our study.

For $\mu_S^2 > 0$, a local minimum can appear in the singlet scalar direction (denoted as v_S^{sym}) before electroweak symmetry breaking (EWSB). For the EW vacuum to be the global minimum after the EWSB, one must have

$$\begin{aligned} V_0(v, 0) < V_0(0, v_S^{\text{sym}}) &\implies \\ \lambda_S > \lambda_H \frac{\mu_S^4}{\mu_H^4} &= \frac{2}{m_H^2 v^2} \left(m_S^2 - \frac{\lambda_{HS}}{2} v^2 \right)^2 \equiv \lambda_S^{\text{min}}. \end{aligned} \quad (6)$$

We take $\{v, m_h, m_S, \lambda_{HS}, \lambda_S\}$ as the input parameter set in favor of the original one, $\{\mu_H^2, \mu_S^2, \lambda_H, \lambda_{HS}, \lambda_S\}$. At the tree level, one gets

$$\mu_H^2 = \frac{m_h^2}{2}, \quad \mu_S^2 = -m_S^2 + \frac{\lambda_{HS}}{2} v^2, \quad \lambda_H = \frac{m_h^2}{2v^2}. \quad (7)$$

In our numerical analyses, we take $\lambda_S = \lambda_S^{\text{min}} + 0.1$ as adopted in Ref. [8].

The tadpole conditions and scalar masses at one-loop level are calculated using [14,25]

$$V_{\text{CW}}(\bar{m}_i^2) = \sum_i n_i \frac{\bar{m}_i^4}{4(16\pi^2)} \left(\ln \frac{\bar{m}_i^2}{\bar{\mu}^2} - c_i \right), \quad (8)$$

which is regularized in the $\overline{\text{MS}}$ scheme, where \bar{m}_i are the background-field-dependent masses of the Higgs bosons ($H_{1,2}$), the NG bosons (G^0, G^\pm), the weak gauge bosons (W, Z) and the top quark (t) with $n_{H_1} = n_{H_2} = n_{G^0} = 1$, $n_{G^\pm} = 2$, $n_W = 6$, $n_Z = 3$, $n_t = -12$, $c = 3/2$ for the scalars and top quark while $c = 5/6$ for the gauge bosons, and $\bar{\mu}$ denotes the renormalization scale. Note that $H_{1,2}$ are the admixtures of h and S occurring for field configurations other than the vacuum.

We first describe the OS-like scheme in which the tree-level relations are not altered by the loop corrections [26].² To this end, the (finite) renormalization conditions are imposed as

$$\begin{aligned} \left\langle \frac{\partial (V_{\text{CW}} + V_{\text{CT}})}{\partial \varphi} \right\rangle &= 0, & \left\langle \frac{\partial^2 (V_{\text{CW}} + V_{\text{CT}})}{\partial \varphi^2} \right\rangle &= 0, \\ \left\langle \frac{\partial^2 (V_{\text{CW}} + V_{\text{CT}})}{\partial \varphi_S^2} \right\rangle &= 0, \end{aligned} \quad (9)$$

where

² For the genuine OS scheme in the SM with the singlet scalar, see, e.g., Ref. [27]

$$V_{\text{CT}} = -\frac{\delta\mu_H^2}{2}\varphi^2 - \frac{\delta\mu_S^2}{2}\varphi_S^2. \quad (10)$$

Note that the conditions (9) also fix $\bar{\mu}$ in addition to $\delta\mu_H^2$ and $\delta\mu_S^2$. As a result, the renormalized one-loop effective potential takes the form

$$V_1^{(\text{OS})}(\varphi, \varphi_S) = \sum_i n_i \frac{1}{4(16\pi^2)} \left[\bar{m}_i^4 \left(\ln \frac{\bar{m}_i^2}{m_i^2} - \frac{3}{2} \right) + 2\bar{m}_i^2 m_i^2 \right], \quad (11)$$

where $m_i^2 = \langle \bar{m}_i^2 \rangle$. In this scheme, the NG bosons cause the IR divergence in the second condition in Eq. (9). To circumvent it, their contributions should be treated with a special care. In this work, we adopt a prescription proposed in Refs. [19,20].³ In this case, the resummed NG contributions take the form

$$V_{\text{CW}}^{(\text{G})}(\varphi) = \frac{\bar{M}_{G^0}^4}{4(16\pi^2)} \left(\ln \frac{\bar{M}_{G^0}^2}{\bar{\mu}^2} - \frac{3}{2} \right) + 2 \cdot \frac{\bar{M}_{G^\pm}^4}{4(16\pi^2)} \left(\ln \frac{\bar{M}_{G^\pm}^2}{\bar{\mu}^2} - \frac{3}{2} \right), \quad (12)$$

where $\bar{M}_{G^{0,\pm}}^2 = \bar{m}_{G^{0,\pm}}^2 + \bar{\Sigma}_G$ with $\bar{\Sigma}_G$ being the one-loop self-energy of the NG bosons with vanishing external momenta,

$$\begin{aligned} \bar{\Sigma}_G = & \frac{1}{16\pi^2} \left[3\lambda_H \bar{m}_{H_1}^2 \left(\ln \frac{\bar{m}_{H_1}^2}{\bar{\mu}^2} - 1 \right) + \frac{1}{2} \lambda_{HS} \bar{m}_{H_2}^2 \left(\ln \frac{\bar{m}_{H_2}^2}{\bar{\mu}^2} - 1 \right) \right. \\ & + \frac{3g_2^2}{2} \bar{m}_W^2 \left(\ln \frac{\bar{m}_W^2}{\bar{\mu}^2} - \frac{1}{3} \right) + \frac{3(g_2^2 + g_1^2)}{4} \bar{m}_Z^2 \left(\ln \frac{\bar{m}_Z^2}{\bar{\mu}^2} - \frac{1}{3} \right) \\ & \left. - 6y_t^2 \bar{m}_t^2 \left(\ln \frac{\bar{m}_t^2}{\bar{\mu}^2} - 1 \right) \right], \quad (13) \end{aligned}$$

where $g_{2,1}$ denote the $SU(2)_L$ and $U(1)_Y$ gauge couplings, respectively, and y_t the top Yukawa coupling. The leading contribution comes from the top quark loop. With this resummation prescription, the second derivative of Eq. (12) evaluated in the vacuum is made finite, $m_{G^{0,\pm}} = 0$.

Now we move on to discuss the one-loop corrected tadpole conditions and Higgs masses in the $\overline{\text{MS}}$ scheme. In this case, we impose

$$T_h = \left\langle \frac{\partial(V_0 + V_{\text{CW}})}{\partial\varphi} \right\rangle = (-\mu_H^2 + \lambda_H v^2)v + \left\langle \frac{\partial V_{\text{CW}}}{\partial\varphi} \right\rangle = 0, \quad (14)$$

$$m_h^2 = \left\langle \frac{\partial^2(V_0 + V_{\text{CW}})}{\partial\varphi^2} \right\rangle = 2\lambda_H v^2 + \left\langle \frac{\partial^2 V_{\text{CW}}}{\partial\varphi^2} \right\rangle - \frac{1}{v} \left\langle \frac{\partial V_{\text{CW}}}{\partial\varphi} \right\rangle, \quad (15)$$

$$m_S^2 = \left\langle \frac{\partial^2(V_0 + V_{\text{CW}})}{\partial\varphi_S^2} \right\rangle = -\mu_S^2 + \frac{\lambda_{HS}}{2} v^2 + \left\langle \frac{\partial^2 V_{\text{CW}}}{\partial\varphi_S^2} \right\rangle. \quad (16)$$

In Eq. (15), μ_H^2 is eliminated by use of Eq. (14). In contrast to the OS-like scheme, m_h does not suffer from the IR divergence since $m_{G^{0,\pm}} \neq 0$ in the vacuum. We determine the parameters $\{\mu_H^2, \mu_S^2, \lambda_H\}$ by solving the above three conditions numerically. In our numerical analyses, $\bar{\mu}$ is varied from $m_t/2$ to $2m_t$ with $m_t = 173.2$ GeV in order to quantify the scale uncertainty.

³ The IR divergence issue can also be cured by using the on-shell Higgs mass rather than the zero-momentum defined Higgs mass [21].

3. Electroweak phase transition

For the EWBG scenario to work, the baryon-changing processes have to be sufficiently suppressed inside the expanding bubbles. The criterion for it is given by

$$\frac{v_C}{T_C} > \zeta_{\text{sph}}(T_C), \quad (17)$$

where $\zeta_{\text{sph}}(T_C)$ depends on the sphaleron configuration [28], the fluctuation determinants about it, and so on [16,29–32]. In the current model, it is found that $\zeta_{\text{sph}} \simeq 1.1\text{--}1.2$ [31], where the one-loop effective potential with thermal resummation is used to evaluate the sphaleron energy. It is thus ξ -dependent and must be revised in a gauge-invariant manner. We defer it to a future study.

To investigate the EWPT, we use the finite- T one-loop effective potential given by [33]

$$V_1^T(\varphi, \varphi_S; T) = \sum_i n_i \frac{T^4}{2\pi^2} I_{B,F} \left(\frac{\bar{m}_i^2}{T^2} \right), \quad (18)$$

$$I_{B,F}(a^2) = \int_0^\infty dx x^2 \ln \left(1 \mp e^{-\sqrt{x^2 + a^2}} \right).$$

Since the perturbative expansion would break down at high temperatures, the dominant thermal pieces must be resummed. In this work, we adopt a prescription such that \bar{m}_i^2 appearing in the thermal function of $I_B(\bar{m}_i^2/T^2)$ are replaced with $\bar{m}_i^2 + \Sigma_i(T)$ with $\Sigma_i(T)$ being the thermal masses (for a refined resummation method, see, e.g., Ref. [9]). The explicit expressions of $\Sigma_i(T)$ can be found in Refs. [7,34]

As pointed out in Ref. [35], two-step phase transitions have expanded EWBG possibilities in models with singlet scalar extensions. In our case, the primary phase transition occurs from $(\varphi, \varphi_S) = (0, 0)$ to $(\varphi, \varphi_S) = (0, v_S^{\text{sym}})$, followed by the secondary transition to $(\varphi, \varphi_S) = (v, v_S^{\text{br}})$. The critical temperature, T_C , of the EWPT in standard gauge-dependent EWPT calculations is defined by the degenerate minima condition

$$V_{\text{eff}}(0, v_S^{\text{sym}}; T_C) = V_{\text{eff}}(v_C, v_S^{\text{br}}; T_C), \quad (19)$$

where $v_C = \lim_{T \uparrow T_C} v(T)$, $v_S^{\text{br}} = \lim_{T \uparrow T_C} v_S(T)$, $v_S^{\text{sym}} = \lim_{T \downarrow T_C} v_S(T)$ with the uparrow (downarrow) being the limit taken from below (above) T_C . We will determine T_C and the VEVs using the effective potential at $T = 0$ with the renormalization conditions explained above and Eq. (18) with the thermal resummation.

In the PRM scheme [16], on the other hand, T_C is determined so as to satisfy the NFK identity expressed by

$$\frac{\partial V_{\text{eff}}(\varphi)}{\partial\xi} = -C(\varphi, \xi) \frac{\partial V_{\text{eff}}(\varphi)}{\partial\varphi}, \quad (20)$$

where $C(\varphi, \xi)$ is some functional. In the perturbative analysis, V_{eff} and $C(\varphi, \xi)$ should be expanded in powers of \hbar :

$$V_{\text{eff}}(\varphi) = V_0(\varphi) + \hbar V_1(\varphi) + \hbar^2 V_2(\varphi) + \dots, \quad (21)$$

$$C(\varphi, \xi) = c_0 + \hbar c_1(\varphi, \xi) + \hbar^2 c_2(\varphi, \xi) + \dots.$$

Since $c_0 = 0$ due to the ξ independence of V_0 , the identity to $\mathcal{O}(\hbar)$ is cast into the form

$$\frac{\partial V_1}{\partial\xi} = -c_1 \frac{\partial V_0}{\partial\varphi}. \quad (22)$$

Therefore, the ξ dependence of V_1 disappears at the stationary points of V_0 rather than those of V_1 .

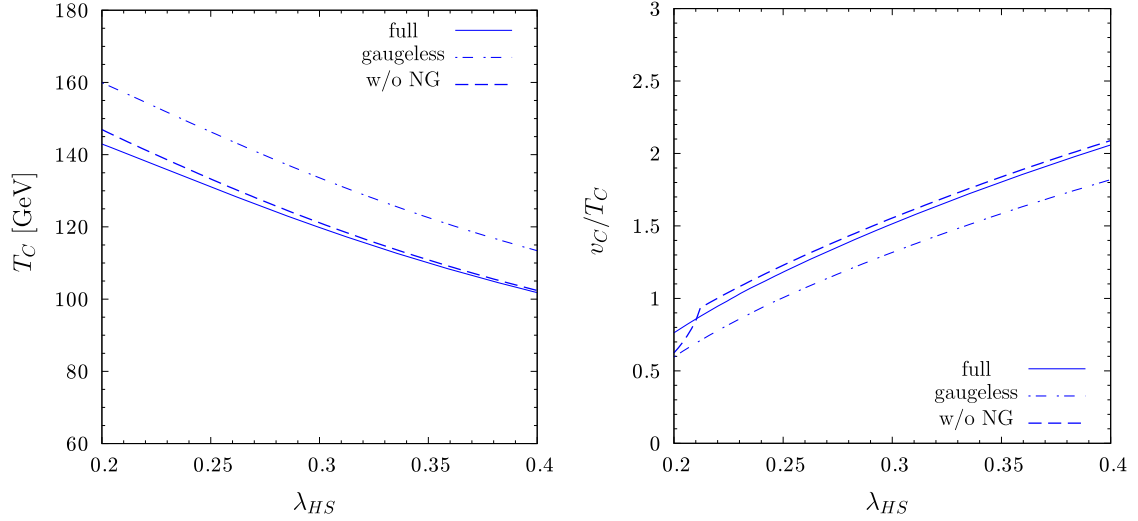


Fig. 1. Impacts of the thermal gauge bosons (dot-dashed curves) and NG bosons (dashed curves) on T_C (left) and v_C/T_C (right) as a function of λ_{HS} . The solid curves include both contributions. Here the OS-like scheme is used.

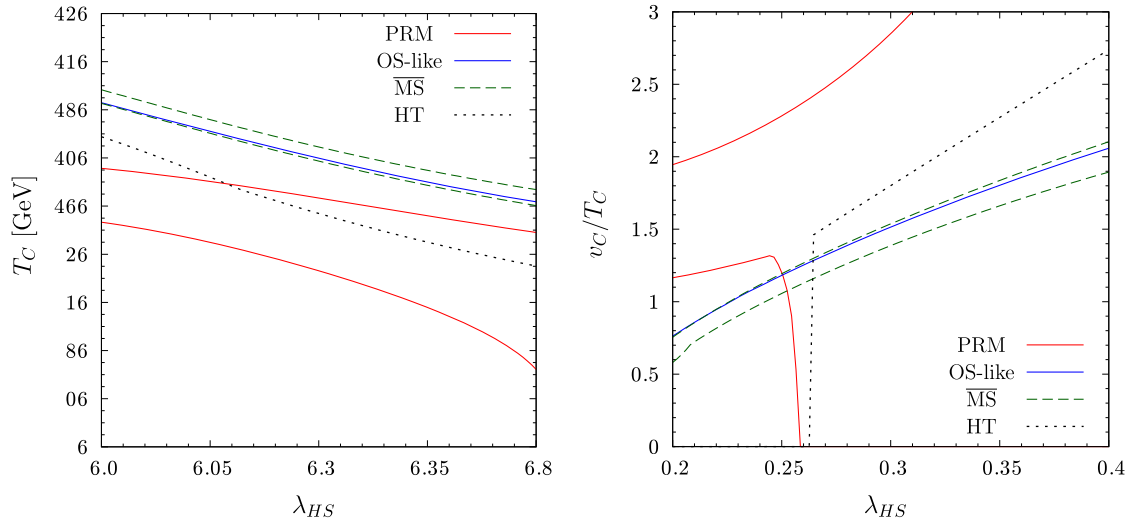


Fig. 2. Comparisons among the various calculation methods: PRM (red-solid), OS-like scheme with the NG resummation (blue-solid), $\overline{\text{MS}}$ (green-dash), and HT (black-dot), respectively. For PRM and $\overline{\text{MS}}$, $\bar{\mu}$ is varied from $m_t/2$ to $2m_t$.

In the aforementioned two-step phase transition case, T_C to $\mathcal{O}(\hbar)$ in the PRM is determined by

$$\begin{aligned} & V_0(0, v_{S,\text{tree}}^{\text{sym}}) + V_{\text{CW}}(0, v_{S,\text{tree}}^{\text{sym}}) + V_1^T(0, v_{S,\text{tree}}^{\text{sym}}; T_C) \\ &= V_0(v_{\text{tree}}, 0) + V_{\text{CW}}(v_{\text{tree}}, 0) + V_1^T(v_{\text{tree}}, 0; T_C), \end{aligned} \quad (23)$$

where $v_{\text{tree}} = 246$ GeV and $v_{S,\text{tree}}^{\text{sym}}$ is the minimum of $V_0(0, \varphi_S)$. Unlike the standard gauge-dependent calculations, the field values are fixed by the tree-level stationary points. As a result, T_C in this scheme becomes lower than those in the gauge-dependent calculations, determined by Eq. (19). It is shown in Ref. [24] that the $\bar{\mu}$ dependence in V_{CW} can affect T_C significantly. This is due to the fact that in the ordinary gauge-dependent methods at one-loop level, the one-loop tadpole conditions, which are $\bar{\mu}$ dependent, are used in determining T_C . As a result, the $\bar{\mu}$ dependences of V_{CW} are partially cancelled. In the PRM method, on the other hand, the tree-level tadpole conditions are used even at the one-loop order in order to satisfy the NFK identity, yielding the larger $\bar{\mu}$ dependences. In Ref. [24], using renormalization group equations, $(V_0 + V_{\text{CW}})$ is made $\bar{\mu}$ -independent up to higher-order corrections. However, we still have degrees of freedom to choose an input scale

for the running parameters to which T_C is vulnerable. The fundamental solution for it may require higher order corrections that are missing here. In the current analysis, we do not elaborate a more refined calculation and just vary $\bar{\mu}$ from $m_t/2$ to $2m_t$ in order to estimate the scale uncertainty of T_C as in the $\overline{\text{MS}}$ scheme.

In the PRM scheme, the VEVs at T_C are determined by the minima of the HT potential defined by

$$V^{\text{HT}}(\varphi, \varphi_S) = V_0(\varphi, \varphi_S) + \frac{1}{2}\Sigma_H(T)\varphi^2 + \frac{1}{2}\Sigma_S(T)\varphi_S^2, \quad (24)$$

where $\Sigma_H(T)$ and $\Sigma_S(T)$ are the thermal masses of H and S , respectively [7]. The HT potential is manifestly ξ independent, thanks to the ξ independence of the thermal masses as mentioned in Introduction. Because of this nice property, it is possible to obtain the gauge-invariant T_C and VEVs by solely using the potential. Application of the HT scheme to the singlet-extended SMs can be found in Ref. [10].

4. Results

Here we conduct the numerical analysis. The free parameters in this model are m_S , λ_{HS} and λ_S . In the current study, we take $m_S = m_h/2$ that is consistent with the DM phenomenology⁴ and $\lambda_S = \lambda_S^{\min} + 0.1$, and thus λ_{HS} is the only parameter we vary. We focus mostly on the parameter space where $v_C/T_C \simeq 1$ realized by the two-step EWPT associate with the tree-level potential barrier. In this case, the range of λ_{HS} is also more or less fixed.

In Fig. 1, we study the EWPT in two approximations. One is the calculation without including the thermal gauge boson loops, denoted as “gaugeless” and depicted by the dot-dashed curves,⁵ and the other is the one without the NG boson contributions, denoted as “w/o NG” and depicted by the dashed curves. The solid curves labeled by “full” includes both of them. Here the OS-like renormalization scheme is adopted. The left and right plots show T_C and v_C/T_C as functions of λ_{HS} , respectively. One can see that the thermal gauge boson loops have a (12–17)% effect on T_C and (12–22)% on v_C/T_C . What is remarkable here is that the importance of the gauge boson loops persists even if the tree-potential barrier exists. As mentioned in Introduction, the figures are not necessarily equivalent to the ξ dependence itself, but it is expected that the larger percentages naively correspond to a greater possibility of the ξ artifact. Formally, the ξ dependence comes from the next order in the perturbative expansion so that its magnitude is not so large as long as ξ is assumed to be an $\mathcal{O}(1)$ parameter, which may not be justified *a priori* though. As discussed in Ref. [36], however, even if the ξ dependence on T_C is a few %, it cannot guarantee that the bubble nucleation temperature or gravitational waves generated during the first-order phase transitions also have similar ξ dependences. Actually, the gravitational wave spectrum in a $U(1)_{B-L}$ model discussed in Ref. [36] can change by one order magnitude when varying ξ from 0 to 5. Having this in mind, the results shown in Fig. 1 motivate us to conduct further investigations in the current model as well. The quantification of the ξ dependence on the EWPT using the general R_ξ gauge will be given elsewhere.

We also find that the NG boson effects are (0.6–2.7)% in T_C and (1.5–18)% in v_C/T_C , respectively. Note that the effect becomes more pronounced if the thermal potential barrier dominates over the tree-level potential barrier, which occurs when $\lambda_{HS} \simeq 0.21$ and below, as shown by the bend in the dashed curve of the right panel. Otherwise, the effect is typically at a few % level.

Now we investigate the scheme dependence using the other methods: PRM, \overline{MS} , and HT schemes. The numerical results are summarized in Fig. 2. The colors and styles of the curves are as follows: PRM scheme (red-solid), OS-like scheme with the NG resummation (blue-solid), \overline{MS} scheme (green-dash), and HT scheme (black-dot). For the PRM and \overline{MS} schemes, $\bar{\mu}$ is varied from $m_t/2$ and $2m_t$. We find the following:

1. The OS-like and \overline{MS} schemes show a nice agreement between each other within the scale uncertainties in the \overline{MS} scheme which are (3.8–6.2)% in T_C and (10–23)% in v_C/T_C , respectively. Here the upper (lower) curve in T_C corresponds to the case with $\bar{\mu} = 2m_t$ ($m_t/2$), and the other way around for v_C/T_C . One can find that the two results get closer if $\bar{\mu} = m_t/2$ is taken. For the commonly used choice in the literature, $\bar{\mu} = m_t$, on the other hand, T_C (v_C/T_C) in the \overline{MS} scheme

is larger (smaller) than that in the OS-like scheme by $\sim 1.5\%$ (2.7–9.5%). In any case, the relatively large scale uncertainties, especially in v_C/T_C in the \overline{MS} scheme indicates the necessity of higher-order corrections.

2. The PRM scheme gives qualitatively the same behavior of T_C against λ_{HS} as in the OS-like and \overline{MS} schemes; namely, T_C gets smaller as λ_{HS} increases. Here the upper (lower) curve in T_C is for $\bar{\mu} = m_t/2$ ($2m_t$), and the other way around for v_C/T_C . One can see that this scheme is subject to more scale uncertainties as mentioned in Sec. 3. In spite of this, one of the universal features of this scheme is that T_C is lower than the gauge-dependent T_C , which is the consequence of the different determination of T_C ; i.e., the degenerate point is away from the minimum of the one-loop effective potential, and hence the degeneracy occurs at a lower T . Because of the lower T_C , v_C/T_C is enhanced compared to those of the OS-like and \overline{MS} schemes except around $\bar{\mu} = m_t/2$, where v_C becomes zero for $\lambda_{HS} \gtrsim 0.25$ since T_C in PRM gets larger than that in HT. Nevertheless, we conclude that there is no significant inconsistency between the PRM and other schemes within the theoretical uncertainties. In any case, a more refined calculation with higher-order corrections such as at $\mathcal{O}(\hbar^2)$ and the daisy diagrams is indispensable for a quantitative analysis.
3. The critical temperature T_C in the HT scheme can be smaller than those in the OS-like and \overline{MS} schemes by about (10–30) GeV. We also find that the EWPT in the HT scheme is not first-order for $\lambda_{HS} \lesssim 0.26$. Moreover, even if it becomes first order, v_C/T_C is overestimated compared to the other two schemes, which signifies the importance of the one-loop corrections.

Before closing this section, we briefly comment on the Landau pole issue in this scenario. In most EWBG scenarios, the region of $v_C/T_C > 1$ is not compatible with the absence of the Landau pole up to the Planck scale ($\sim 10^{19}$ GeV). In the above scenario, in contrast, it is found that all the couplings in the model are less than 4π all the way to the Planck scale for $\lambda_{HS} \lesssim 0.33$ using the one-loop renormalization group equations.

5. Conclusion and discussions

We have revisited EWPT in the singlet-extended SM using several calculation methods to study the scheme dependence. In the OS-like scheme, the NG bosons must be taken with a special care in order to avoid the IR divergence. Here we adopted the NG resummation method recently proposed in Refs. [19,20] and quantified such a resummation effect on first-order EWPT. It is found that the effect can get pronounced if the potential barrier is governed mainly by the thermal cubic loops rather than the tree-potential structure. If not, the effect is typically at $\sim 1\%$ level. In addition, we numerically studied the impacts of the thermal gauge boson loops on v_C/T_C and found that such loops had a (12–22)% effect on v_C/T_C even when the tree-level potential barrier existed. This motivates us to conduct the precise quantification of the ξ dependence using the general R_ξ gauge in a future study.

We also found that the results in the OS-like and \overline{MS} schemes showed a nice agreement within the scale uncertainties which are (3.8–6.2)% in T_C and (10–23)% in v_C/T_C . Our numerical studies also clarified that T_C and the corresponding VEVs against λ_{HS} in the gauge-invariant PRM method were qualitatively consistent with those in the above gauge-dependent schemes within the rather large theoretical uncertainties. Regardless of the gauge-dependent or -independent methods, we found that the scale uncertainties

⁴ It is well known that the DM relic density is lower than the observed value in parameter space consistent with the strong first-order EWPT. For a recent study of DM in this model, see, e.g., Ref. [12].

⁵ We have confirmed that the zero temperature gauge boson loops have little effect on EWPT.

in v_C/T_C were more than about 10%, suggesting that higher-order corrections could be potentially important.

Acknowledgements

This work was supported in part by the Ministry of Science and Technology of Taiwan under Grant Nos. 104-2628-M-008-004-MY4 and 104-2811-M-008-056, and Institute for Basic Science under the project code, IBS-R018-D1.

References

- [1] C. Patrignani, et al., Particle Data Group, *Chin. Phys. C* 40 (10) (2016) 100001.
- [2] A.D. Sakharov, *Pisma Zh. Eksp. Teor. Fiz.* 5 (1967) 32, *JETP Lett.* 5 (1967) 24, *Sov. Phys. Usp.* 34 (5) (1991) 392, *Usp. Fiz. Nauk* 161 (5) (1991) 61.
- [3] G. Aad, et al., ATLAS Collaboration, *Phys. Lett. B* 716 (2012) 1; S. Chatrchyan, et al., CMS Collaboration, *Phys. Lett. B* 716 (2012) 30.
- [4] V.A. Kuzmin, V.A. Rubakov, M.E. Shaposhnikov, *Phys. Lett. B* 155 (1985) 36; For reviews on electroweak baryogenesis, see A.G. Cohen, D.B. Kaplan, A.E. Nelson, *Annu. Rev. Nucl. Part. Sci.* 43 (1993) 27; M. Quiros, *Helv. Phys. Acta* 67 (1994) 451; V.A. Rubakov, M.E. Shaposhnikov, *Usp. Fiz. Nauk* 166 (1996) 493; K. Funakubo, *Prog. Theor. Phys.* 96 (1996) 475; M. Trodden, *Rev. Mod. Phys.* 71 (1999) 1463; W. Bernreuther, *Lect. Notes Phys.* 591 (2002) 237; J.M. Cline, arXiv:hep-ph/0609145; D.E. Morrissey, M.J. Ramsey-Musolf, *New J. Phys.* 14 (2012) 125003; T. Konstandin, *Phys. Usp.* 56 (2013) 747, *Usp. Fiz. Nauk* 183 (2013) 785.
- [5] K. Kajantie, M. Laine, K. Rummukainen, M.E. Shaposhnikov, *Phys. Rev. Lett.* 77 (1996) 2887; K. Rummukainen, M. Tsypin, K. Kajantie, M. Laine, M.E. Shaposhnikov, *Nucl. Phys. B* 532 (1998) 283; F. Csikor, Z. Fodor, J. Heitger, *Phys. Rev. Lett.* 82 (1999) 21; Y. Aoki, F. Csikor, Z. Fodor, A. Ukawa, *Phys. Rev. D* 60 (1999) 013001.
- [6] J.R. Espinosa, M. Quiros, *Phys. Rev. D* 76 (2007) 076004; S. Profumo, M.J. Ramsey-Musolf, G. Shaughnessy, *J. High Energy Phys.* 0708 (2007) 010; D.J.H. Chung, A.J. Long, L.T. Wang, *Phys. Rev. D* 87 (2) (2013) 023509; N. Craig, H.K. Lou, M. McCullough, A. Thalappilil, *J. High Energy Phys.* 1602 (2016) 127; S. Ghosh, A. Kundu, S. Ray, *Phys. Rev. D* 93 (11) (2016) 115034; T. Tenkanen, K. Tuominen, V. Vaskonen, *J. Cosmol. Astropart. Phys.* 1609 (09) (2016) 037; P.H. Ghorbani, *J. High Energy Phys.* 1708 (2017) 058; L. Marzola, A. Racioppi, V. Vaskonen, *Eur. Phys. J. C* 77 (7) (2017) 484; G. Kurup, M. Perelstein, *Phys. Rev. D* 96 (1) (2017) 015036; B. Jain, S.J. Lee, M. Son, arXiv:1709.03232 [hep-ph]; K. Ghorbani, P.H. Ghorbani, arXiv:1804.05798 [hep-ph].
- [7] J.R. Espinosa, T. Konstandin, F. Riva, *Nucl. Phys. B* 854 (2012) 592.
- [8] D. Curtin, P. Meade, C.T. Yu, *J. High Energy Phys.* 1411 (2014) 127.
- [9] D. Curtin, P. Meade, H. Ramani, arXiv:1612.00466 [hep-ph].
- [10] V. Vaskonen, *Phys. Rev. D* 95 (12) (2017) 123515.
- [11] V. Silveira, A. Zee, *Phys. Lett. B* 161 (1985) 136; J. McDonald, *Phys. Rev. D* 50 (1994) 3637; C.P. Burgess, M. Pospelov, T. ter Veldhuis, *Nucl. Phys. B* 619 (2001) 709; D. O'Connell, M.J. Ramsey-Musolf, M.B. Wise, *Phys. Rev. D* 75 (2007) 037701; V. Barger, P. Langacker, M. McCaskey, M.J. Ramsey-Musolf, G. Shaughnessy, *Phys. Rev. D* 77 (2008) 035005; M. Gonderinger, Y. Li, H. Patel, M.J. Ramsey-Musolf, *J. High Energy Phys.* 1001 (2010) 053; W.L. Guo, Y.L. Wu, *J. High Energy Phys.* 1010 (2010) 083; A. Bandyopadhyay, S. Chakraborty, A. Ghosal, D. Majumdar, *J. High Energy Phys.* 1011 (2010) 065; S. Profumo, L. Ubaldi, C. Wainwright, *Phys. Rev. D* 82 (2010) 123514; Y. Mambrini, *Phys. Rev. D* 84 (2011) 115017; A. Biswas, D. Majumdar, *Pramana* 80 (2013) 539; J.M. Cline, K. Kainulainen, P. Scott, C. Weniger, *Phys. Rev. D* 88 (2013) 055025, *Phys. Rev. D* 92 (3) (2015) 039906 (Erratum); A. Falkowski, C. Gross, O. Lebedev, *J. High Energy Phys.* 1505 (2015) 057; S. Bhattacharya, P. Poulose, P. Ghosh, *J. Cosmol. Astropart. Phys.* 1704 (04) (2017) 043; J.A. Casas, D.G. Cerdeño, J.M. Moreno, J. Quilis, *J. High Energy Phys.* 1705 (2017) 036.
- [12] P. Athron, et al., GAMBIT Collaboration, *Eur. Phys. J. C* 77 (8) (2017) 568; P. Athron, J.M. Cornell, F. Kahlhoefer, J. McKay, P. Scott, S. Wild, arXiv:1806.11281 [hep-ph].
- [13] S. Das, P.J. Fox, A. Kumar, N. Weiner, *J. High Energy Phys.* 1011 (2010) 108; D.J.H. Chung, A.J. Long, *Phys. Rev. D* 84 (2011) 103513; J.M. Cline, K. Kainulainen, *J. Cosmol. Astropart. Phys.* 1301 (2013) 012; J.M. Cline, K. Kainulainen, P. Scott, C. Weniger, *Phys. Rev. D* 88 (2013) 055025, *Phys. Rev. D* 92 (3) (2015) 039906 (Erratum); T. Alanne, K. Tuominen, V. Vaskonen, *Nucl. Phys. B* 889 (2014) 692; M. Chala, G. Nardini, I. Sobolev, *Phys. Rev. D* 94 (5) (2016) 055006.
- [14] R. Jackiw, *Phys. Rev. D* 9 (1974) 1686.
- [15] L. Dolan, R. Jackiw, *Phys. Rev. D* 9 (1974) 2904.
- [16] H.H. Patel, M.J. Ramsey-Musolf, *J. High Energy Phys.* 1107 (2011) 029.
- [17] M. Garny, T. Konstandin, *J. High Energy Phys.* 1207 (2012) 189.
- [18] C.L. Wainwright, S. Profumo, M.J. Ramsey-Musolf, *Phys. Rev. D* 86 (2012) 083537.
- [19] S.P. Martin, *Phys. Rev. D* 90 (1) (2014) 016013.
- [20] J. Elias-Miro, J.R. Espinosa, T. Konstandin, *J. High Energy Phys.* 1408 (2014) 034.
- [21] J.M. Cline, P.A. Lemieux, *Phys. Rev. D* 55 (1997) 3873; C. Delaunay, C. Grojean, J.D. Wells, *J. High Energy Phys.* 0804 (2008) 029; J.M. Cline, K. Kainulainen, M. Trott, *J. High Energy Phys.* 1111 (2011) 089.
- [22] N.K. Nielsen, *Nucl. Phys. B* 101 (1975) 173.
- [23] R. Fukuda, T. Kugo, *Phys. Rev. D* 13 (1976) 3469.
- [24] C.W. Chiang, M.J. Ramsey-Musolf, E. Senaha, *Phys. Rev. D* 97 (1) (2018) 015005.
- [25] S.R. Coleman, E.J. Weinberg, *Phys. Rev. D* 7 (1973) 1888; S. Weinberg, *Phys. Rev. D* 7 (1973) 2887.
- [26] D.A. Kirzhnits, A.D. Linde, *Ann. Phys.* 101 (1976) 195.
- [27] S. Kanemura, M. Kikuchi, K. Yagyu, *Nucl. Phys. B* 917 (2017) 154; S. Kanemura, M. Kikuchi, K. Sakurai, K. Yagyu, *Phys. Rev. D* 96 (3) (2017) 035014; G. Ria, D. Meloni, *Eur. Phys. J. C* 78 (3) (2018) 270.
- [28] N.S. Manton, *Phys. Rev. D* 28 (1983) 2019; F.R. Klinkhamer, N.S. Manton, *Phys. Rev. D* 30 (1984) 2212.
- [29] A. Hriche, *Phys. Rev. D* 75 (2007) 083522.
- [30] K. Funakubo, E. Senaha, *Phys. Rev. D* 79 (2009) 115024.
- [31] K. Fuyuto, E. Senaha, *Phys. Rev. D* 90 (1) (2014) 015015.
- [32] A. Hriche, T.A. Chowdhury, S. Nasri, *J. High Energy Phys.* 1411 (2014) 096.
- [33] L. Dolan, R. Jackiw, *Phys. Rev. D* 9 (1974) 3320.
- [34] M.E. Carrington, *Phys. Rev. D* 45 (1992) 2933.
- [35] K. Funakubo, S. Tao, F. Toyoda, *Prog. Theor. Phys.* 114 (2005) 369.
- [36] C.W. Chiang, E. Senaha, *Phys. Lett. B* 774 (2017) 489.